Non-linear statics and dynamics of nanoelectromechanical systems based on nanoplates and nanowires

N Pugno
Department of Structural Engineering, Politecnico di Torino, Corso Duca degli Abruzzi 24, Torino 10129, Italy.
email: nicola.pugno@polito.it

The manuscript was received on 10 June 2004 and was accepted after revision for publication on 24 May 2005.

DOI: 10.1243/174034905X55953

Abstract: An analysis of three-dimensional nanoelectromechanical systems (NEMS) is presented. Nanotubes could be a key one-dimensional element in future NEMS devices; but they would be inadequate when two- or three-dimensional structures are required. A general free-energy-based formulation to treat statics and dynamics of three-dimensional NEMS, according to classical or quantum mechanics, is derived and presented; the method is then applied to nanoplates and nanowires. The equilibrium and stability of an elastic (e.g., graphene sheet) nanoplate-based NEMS under an electrical field and van der Waals forces (Pauli's repulsion and large displacements are also discussed) are evaluated by minimizing the free energy and by the sign of the determinant of its Hessian matrix. The structural instability, arising at the so-called pull-in voltage, would correspond to the switch of the device. The amplitude and frequency of the thermal vibrations of the nanoplate are evaluated as a function of the applied voltage. The effect of the van der Waals forces on the NEMS dynamics is also presented. The amplitude and frequency of the oscillations at 0 K, from the uncertainty principle, are estimated.

Keywords: nanoelectromechanical systems, nanoplates, nanowires, pull-in voltage, vibrations

1 INTRODUCTION

Microelectromechanical systems (MEMS) – devices with size of the order of a micrometer – have already had a strong impact on different technology areas. The natural evolution of these systems is their miniaturization towards nanoelectromechanical systems (NEMS), having a characteristic size of the order of a nanometer. The potential for NEMS is tremendous, reaching an integration level of the order of 10^{12} elements/cm^2 and frequency in the GHz band [**1–3**].

NEMS are about three orders of magnitude smaller than MEMS; and therefore new effects have to be taken into account, as demonstrated for nanotube-based NEMS [**4**], for example, thermal vibrations (which will have a stronger influence on NEMS than MEMS), as well as van der Waals forces, Heisenberg's, and Pauli's principles, which can be (largely) neglected when designing MEMS. Therefore, also the Casimir's force (a purely quantum-mechanical effect arising from the zero-point energy, thus from the Heisenberg's principle) could also have a significant role in the world of the nanosystems.

At large size scale, one- and two-dimensional structures, e.g., tubes and plates, are extensively used in the design of mechanical components. Correspondingly, a strong impact of nanotubes, nanowires, and nanoplates can be expected in the design of NEMS devices. Even if nanotubes have been widely analysed in the last decade, much remains to do on nanowires and nanoplates and in general on three-dimensional nanostructures. Carbon is an interesting material for NEMS design, because of its excellent electronic and mechanical properties [**5**], as clearly shown by the numerous analyses carried out on carbon nanotubes during the last decade, after their discovery by Iijima [**6**]. In this paper it is assumed that the mechanical strength of the NEMS is large enough. For its strength prediction quantized fracture mechanics could be applied [**7**].

Since carbon seems to be a key element for MEMS and NEMS applications, after a general treatment,

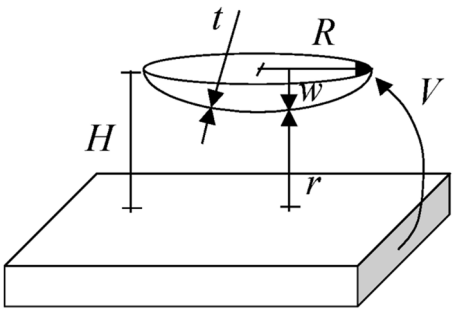

Fig. 1 Elastic nanoplate and grounded rigid plane under electrostatic and van der Waals forces

attention is focused on the structural behaviour of carbon nanoplates, such as graphene sheets (an individual layer of graphite).

The structural behaviour of nanostructures is usually analysed experimentally by scanning electron and atomic force microscopy techniques, numerically by molecular mechanics or dynamics simulations, as well as theoretically by continuum mechanics. Continuum theories seem to be very robust even considering structures with size in the nanometer range [**8**]. Similarly, it has been shown [**9**, **10**] that a continuum model can be used to calculate the van der Waals energy, instead of only the discrete approach based on the attractive term of the Lennard–Jones potential. The same consideration could be extended to the repulsive term, that essentially represents the Pauli's repulsion.

Figure 1 shows the analysed system consisting of an elastic vibrating nanoplate at a given temperature, and a rigid semi-infinite ground plane. The static case of a nanotube suspended over an electrode was numerically analysed in [**10**], as well as theoretically in [**4**] also considering the dynamic and finite kinematic (large displacement) regimes. When a potential difference is created between the nanoplate and the ground plane, electrostatic charges are induced on both structures. The opposite charges give rise to attractive electrostatic forces. In addition, van der Waals attractive forces also act between the two structures. The elastic stiffness of the nanoplate counteracts the attractive electrostatic and van der Waals forces so that an equilibrium position is reached. However, around this equilibrium position, the NEMS is always oscillating as a consequence of thermal vibration.

When the applied potential difference between the nanoplate and the ground plane reaches a certain value, the nanoplate becomes unstable and collapses onto the ground plane. For NEMS it could correspond to an ON state so that when the nanoplate and the ground plane are separated the device is in the OFF state. The potential that causes the nanoplate to collapse onto the ground plane is defined as the *pull-in voltage*. If the gap between the nanoplate and the ground plane is very small, even without an applied voltage, the nanoplate can collapse onto the ground plane because of the van der Waals forces. The Pauli's repulsion plays the role of a mechanical contact. If the elastic opposing force is not sufficient to recover the relaxed configuration, the collapsed configuration is maintained even after the applied voltage is removed; thus, irreversible sticking of NEMS becomes an increasing problem at the nanoscale and can limit the range of operability and the size of NEMS [**10**]. On the other hand, for some applications, the sticking of the nanodevice could be a desired effect (e.g., in acceleration or mass nanosensors – to be used only one time).

In describing the behaviour of NEMS, dynamic effects could play a fundamental role. In particular, important parameters are the amplitude and frequency of the vibrations (e.g., thermal, free, or from zero point vibrations even at 0 K) of the NEMS, as a function of the applied voltage imposed to control the device, and including the effect of the van der Waals forces. A dynamic analysis to estimate these parameters concludes the paper. The use of the equipartition theorem to treat thermal vibrations will be emphasized [**11**].

The paper represents an extension to nanoplates and nanowires of the analytical analysis on nanotubes carried out in [**4**]. The results are analytical formulae to estimate oscillations and instability (pull-in voltage) of the NEMS; they represent a clear advantage with respect to the results obtained by classical numerical approaches (e.g., FEMLAB).

2 ELECTRICAL FIELD, VAN DER WAALS FORCES, AND PAULI'S REPULSION

The electrostatic forces between two oppositely charged structures can be computed by using a standard capacitance model assuming perfect conductors. This implies that the electrostatic potential is constant in the two structures. The electrostatic energy is given by

$$E_{\text{elec}} = \tfrac{1}{2} C V^2 \tag{1}$$

where V is the difference in voltage and C is the capacitance, defined as $C = Q/V$, $\mp Q$ being the two opposite charges in the two conductors. For a double-layer conductor, the contribution to the capacitance of two infinitesimal surfaces $\mathrm{d}S$ oppositely charged and separated by a distance r, is $\mathrm{d}C = \varepsilon_0 \, \mathrm{d}S/r$ where $\varepsilon_0 = 8.85 \times 10^{-12} \, \mathrm{C}^2 \, \mathrm{N}^{-1} \, \mathrm{m}^{-2}$ is the vacuum permittivity.

The van der Waals energy can be computed by using the well-known Lennard–Jones potential,

which has an attractive term ($\propto r^{-6}$, owing to the van der Waals forces) and a repulsive term ($\propto r^{-12}$, basically owing to the Pauli's repulsion). To compute the total van der Waals energy a continuum model can be employed [**9**, **10**]. In the continuum model, the total van der Waals energy is computed by the double-volume integral of the Lennard–Jones potential

$$E_{\mathrm{vdW}} = \int_{V_1}\int_{V_2} \frac{n_1 n_2 C_6}{r^6}\,\mathrm{d}V_1\,\mathrm{d}V_2 \tag{2}$$

where V_1 and V_2 represent the two domains of integration, n_1 and n_2 are the corresponding atom densities, and r is the distance between any point on V_1 and any point on V_2. C_6 is a constant (for example, for the carbon–carbon interaction it is equal to $C_6 = 15.2\,\mathrm{eV\,\mathring{A}}^6 = 2.43 \times 10^{-78}\,\mathrm{N\,m}^7$).

The same approach can be applied to compute the repulsive energy

$$E_{\mathrm{P}} = \int_{V_1}\int_{V_2} \frac{n_1 n_2 C_{12}}{r^{12}}\,\mathrm{d}V_1\,\mathrm{d}V_2 \tag{3}$$

where C_{12} is a constant.

3 FREE ENERGY, EQUILIBRIUM, AND INSTABILITY

The elastic displacements u, v, w (along x, y, and z orthogonal axes of a reference system) of the three-dimensional nanostructure are approximated by a linear combination of a sufficient number N of opportune (e.g., satisfying the boundary conditions) arbitrary functions u_i, v_i, w_i, and unknown constants c_i, representing the displacements of some characteristic points (e.g., some atoms of the lattice) having coordinates (x_i, y_i, z_i)

$$\begin{aligned} u(x,y,z) &= \sum_{i=1}^{Q} c_i u_i(x,y,z) \\ v(x,y,z) &= \sum_{i=Q+1}^{M} c_i v_i(x,y,z) \\ w(x,y,z) &= \sum_{i=M+1}^{N} c_i w_i(x,y,z) \end{aligned} \tag{4}$$

For given constitutive laws (e.g., linear elastic material) the elastic energy stored in the nanostructure is a function only of the displacements or, according to equation (4), of the unknowns c_i

$$E_{\mathrm{elast}} = E_{\mathrm{elast}}(u,v,w) = E_{\mathrm{elast}}(c_i) \tag{5}$$

For example, for linear elastic material $E_{\mathrm{elast}} = \frac{1}{2}\bar{\varepsilon}[\mathrm{H_E}]\varepsilon$ with $[\mathrm{H_E}]$ a constant matrix (the Hessian of the potential elastic energy that describes the stiffness of the material), and $\bar{\varepsilon}$ the strain vector, having the six significant components of the symmetric strain tensor $[\varepsilon]$. The tensor can be obtained directly from the displacements as $[\varepsilon] = \frac{1}{2}([\mathrm{J}] + [\mathrm{J}]^T)$, where $[\mathrm{J}]$ is the Jacobian matrix of u,v,w with respect to x, y, z; for details see [**12**].

The free energy $W(c_i)$ of the NEMS must be written as [**4**]

$$W(c_i) = E_{\mathrm{elast}}(c_i) - E_{\mathrm{elec}}(c_i) - E_{\mathrm{vdW}}(c_i) - E_P(c_i) \tag{6}$$

where all four energies on the right-hand side (and thus also the free energy) are functions only of the unknowns c_i. The integrals in equations (1) to (3) can be computed according to the displacements described by equation (4), in which only the constants c_i survive.

The equilibrium condition will be reached when the free energy reaches a minimum value, thus when the gradient of the free energy, with respect to the unknowns c_i, has vanishing components

$$\bar{\nabla} W = \bar{0}; \qquad (\bar{\nabla} W)_j = \frac{\partial W(c_i)}{\partial c_j}, \quad \forall c_j \quad j = 1, \ldots, N \tag{7}$$

This represents a system of N equations in the N unknowns c_i. From equation (7) the static equilibrium configuration can be derived.

On the other hand, more important than the equilibrium in this study is the prediction of the instability of the system (governing the switch of the NEMS); the voltage corresponding to this instability, the so-called pull-in voltage, represents in fact the key parameter in the design of NEMS. The system will lose its stability when the Hessian matrix $[\mathrm{H_W}]$ of the free-energy (evaluated at the equilibrium position) becomes equal to zero

$$\begin{aligned} &\det[\mathrm{H_W}] = 0; \\ &(\mathrm{H_W})_{jk} = \frac{\partial^2 W(c_i)}{\partial c_j \partial c_k}, \quad \forall c_j, c_k \quad j,k = 1, \ldots, N \end{aligned} \tag{8}$$

From equation (8), the pull-in voltage of the system can be derived.

4 VIBRATIONS AROUND A DEFORMED CONFIGURATION

Consider a second-order Taylor's expansion of the free energy around the equilibrium position. Assuming the free energy to be zero at the equilibrium (arbitrary constant) and noting that at the equilibrium

equation (7) must hold, the expansion can be written as

$$W \approx \tfrac{1}{2}\Delta\bar{c}_{\mathrm{D}}^{T}[\mathrm{H_W}]\,\Delta\bar{c}_{\mathrm{D}} \tag{9}$$

where $(\Delta\bar{c}_{\mathrm{D}})_i = c_{\mathrm{D}i} - c_i$ and the coefficients $c_{\mathrm{D}i}$ describe the dynamic positions of the system (the coefficients c_i refer to statics). The static equilibrium imposed by equation (7) is identical with $[\mathrm{H_W}]\,\Delta\bar{c}_{\mathrm{D}} = \bar{0}$. For the fundamental frequency vibrations around the equilibrium position (neglecting the damping)

$$c_{\mathrm{D}i}(t) \cong c_i + \Delta c_{\mathrm{D}i}(t) = c_i + \Delta c^{*}_{\mathrm{D}i}\sin\omega t, \qquad i = 1, \ldots, N \tag{10}$$

where $\Delta c^{*}_{\mathrm{D}i}$ are the amplitudes of the vibrations around the equilibrium position described by the coefficients c_i at the fundamental frequency ω. The kinetic energy of the system is $K \approx \frac{1}{2}\Delta\dot{\bar{c}}_{\mathrm{D}}^{T}[\mathrm{M}]\,\Delta\dot{\bar{c}}_{\mathrm{D}}$, where [M] is the mass matrix of the system. Thus, the dynamic equations around a deformed configuration can be written as

$$[\mathrm{M}]\Delta\ddot{\bar{c}}_{\mathrm{D}} + [\mathrm{H_W}]\Delta\bar{c}_{\mathrm{D}} = \bar{0} \tag{11}$$

from which the natural frequencies can be derived by the following condition

$$\det([\mathrm{H_W}] - \omega^2[\mathrm{M}]) = 0 \tag{12}$$

Equation (11) is for NEMS dynamics under a deformed configuration according to classical mechanics. The matrix $[\mathrm{H_W}]$ includes not only the elasticity of the system (stiffness matrix) but also the effects of the external fields around the equilibrium position. By the eigenvectors of equation (11), the classical variable substitution to *normal coordinates*, i.e. $\Delta\bar{c}_{\mathrm{D}} \to \bar{\eta}$, allow equation (11) to be placed in the decoupled *canonical form* (in which the matrixes become symmetric). For each normal oscillator, Schrödinger's equation is

$$\left(-\frac{\hbar^2}{2m_i}\frac{\mathrm{d}^2}{\mathrm{d}\eta_i^2} + W_i(\eta_i)\right)\psi_{\mathrm{in}}(\eta_i) = E_{\mathrm{in}}\psi_{\mathrm{in}}(\eta_i) \tag{13}$$

where E_{in} are the energy eigenvalues and ψ_{in} are the eigenfunctions describing the fundamental vibrational states of the normal oscillator i with associated modal mass m_i and free-energy W_i. Assuming the expansion of equation (9) for the free energy associated with the normal coordinates (with frequencies $\omega_{i\eta}$), equation (13) represents the well-known quantum harmonic oscillator and the solution gives the discrete quantized energy levels

$$E_{\mathrm{in}} \approx (\tfrac{1}{2} + n)\hbar\omega_{i\eta} \tag{14}$$

The zero point energy (as imposed by Heisenberg's principle) is

$$E_{i0} \approx \frac{\hbar\omega_{i\eta}}{2} \tag{15}$$

With the kinetic energy at 0 K given by equation (15), the normal amplitude of the 0 K oscillations can be deduced; thus after the inverse transformation $\bar{\eta} \to \Delta\bar{c}_{\mathrm{D}}$ the oscillation amplitudes of the NEMS are estimated. To study the oscillations at temperature T when the vibrational energy level spacing is small compared with $k_{\mathrm{B}}T$ the equipartition theorem has to be applied: each degree of freedom posses kinetic energy $E_{i0} \approx k_{\mathrm{B}}T/2$. After giving the differential equations of the nanoplate in the next section, instead of solving them numerically, in sections 6 and 7 the previous approach is applied to make quantitative predictions for describing the behaviour of nanoplate-based NEMS.

5 DIFFERENTIAL EQUATIONS OF THE NANOPLATE-BASED NEMS

Assume a nanoplate placed on an x–y plane (having a small thickness along z). The electrostatic, van der Waals, and repulsive (Pauli's) forces can be obtained by deriving the corresponding energy terms (1), (2) and (3) with respect to the elastic gap r, the nominal gap is H, see Fig. 1

$$F_{\mathrm{elec,vdW,P}} = -\frac{\mathrm{d}E_{\mathrm{elec,vdW,P}}}{\mathrm{d}r} \tag{16}$$

Consequently, the forces per unit surface area S will be

$$q_{\mathrm{elec,vdW,P}} = \frac{\mathrm{d}F_{\mathrm{elec,vdW,P}}}{\mathrm{d}S} \tag{17}$$

The deflection $w(x, y)$ (the correct one, without assuming the approximation of equation (4)) for a linear elastic isotropic nanoplate are obtained by solving the equation of plates (see, for example, [**13**])

$$D\nabla^4 w - q_{\mathrm{elec}}(w) - q_{\mathrm{vdW}}(w) - q_P(w) = F_{,yy}w_{,xx} + F_{,xx}w_{,yy} - 2F_{,xy}w_{,xy} - \mu w_{,\tau} \tag{18a}$$

$$\nabla^4 F = Et(w_{,xy}^2 - w_{,xx} - w_{,yy}) \tag{18b}$$

$$N_{xx} = F_{,yy}, N_{yy} = F_{,xx}, N_{xy} = -F_{,xy} \tag{18c}$$

with $D = Et^3/12(1-\nu^2)$, where E, ν are the Young's modulus and the Poisson's ratio respectively and t is the nanoplate thickness.

The right-hand side of equation (18a) describes the membrane regime and the inertia of the plate (μ is the mass per unit area and τ is the time; the symbol ',' represents the derivation operator). If the membrane regime and the inertia are neglected, equation (18a) corresponds the well-known Sophie

Germain equation, describing the static flexural regime of the plate. In this case the axial loads (per unit length) N_{xx}, N_{yy}, N_{xy} can be neglected. In general, equations (18a) and (18b) are two coupled equations in the unknowns w and F (this function is connected to the axial loads as reported in equation (18c)). Equations (18) could be solved numerically (e.g., with finite differences, finite element methods, etc.).

The Pauli's repulsion decays extremely fast and is important only when the structures come into contact ($r/H \to 0$), so that, neglecting such contact we can here assume $q_P \approx 0$. The electrostatic and van der Waals energies per unit surface, according to equations (1) and (2) are respectively [**10**]

$$\frac{\mathrm{d}E_{\mathrm{elec}}}{\mathrm{d}S} = \frac{1}{2}\varepsilon_0 \frac{V^2}{r} \tag{19}$$

$$\frac{\mathrm{d}E_{\mathrm{vdW}}}{\mathrm{d}S} = \frac{\pi C_6 n^2}{12}\left(\frac{1}{r^2} - \frac{1}{(r+t)^2}\right) \tag{20}$$

and consequently, from equations (16) and (17), the forces per unit area S acting on the nanoplate are

$$q_{\mathrm{elec}} = \frac{\varepsilon_0 V^2}{2r^2} \tag{21}$$

$$q_{\mathrm{vdW}} = \frac{\pi C_6 n^2}{6}\left(\frac{1}{r^3} - \frac{1}{(r+t)^3}\right) \tag{22}$$

where n is the atomic density (e.g., for graphite it is equal to $n = 1.14 \times 10^{29}\,\mathrm{m}^{-3}$) and for a single monolayer of graphite (graphene) $t = 0.335\,\mathrm{nm}$). Introducing equations (21) and (22) into equation (18) allow us to study the deflection of the nanoplate. As for nanotubes [**10**] it is shown that also for nanoplate the van der Waals contribution becomes predominant as the size of the NEMS decreases: by scaling each characteristic length of the system by a factor of l in equation (6), the electrostatic contribution scales as $F_{\mathrm{elec}} \propto q_{\mathrm{elec}} l^2 \propto l^0$ and the van der Waals contribution scales as $F_{\mathrm{vdW}} \propto q_{\mathrm{vdW}} l^2 \propto l^{-1}$.

6 APPROXIMATED SOLUTION FOR EQUILIBRIUM AND INSTABILITY

6.1 Circular nanoplates

Instead of a numerical study of equation (18), the author prefers to obtain an analytical solution for the deflection w under simplified hypotheses, following the proposed procedure described in sections 2 and 3. To simplify the problem (to treat it in a simple analytical way) (a) it is assumed that the nanoplate thickness t is much smaller than the distance r between nanoplate and ground plane, i.e. $t/r \ll 1$; (b) in the Taylor's expansions of the energy terms, only the first two significant terms are considered to capture the equilibrium and instability of the nanoplate; (c) only one unknown $c_i \equiv c$ is considered when describing the position of the structure; and (d) the Pauli's repulsion is neglected.

As a consequence of (a), considering that $H > r = H - w$, the nanoplate deflection w must be much smaller than the gap H, i.e., $w/H \ll 1 - t/H \cong 1$. Assuming $t/r \ll 1$ and $w/H \ll 1$ (a), as a consequence of (b), equations (19) and (20) become

$$\frac{\mathrm{d}E_{\mathrm{elec}}}{\mathrm{d}S} \approx \frac{\varepsilon_0 V^2}{2H}\left(1 + \frac{w}{H} + \left(\frac{w}{H}\right)^2\right) \tag{23}$$

$$\frac{\mathrm{d}E_{\mathrm{vdW}}}{\mathrm{d}S} = \frac{\pi C_6 n^2 t}{6r^3} \approx \frac{\pi C_6 n^2 t}{6H^3}\left(1 + 3\frac{w}{H} + 6\left(\frac{w}{H}\right)^2\right) \tag{24}$$

Let us focus our attention on a circular nanoplate, for which $w = w(\rho)$, with ρ radial coordinate with respect to the centre of the nanoplate. For example, free-rotating boundary conditions are assumed, for which an approximated solution is searched in the form, according to (c)

$$w(\rho) \approx c\left(1 - \frac{\rho^2}{R^2}\right) \tag{25}$$

where R is the radius of the nanoplate, and c is the unknown constant, i.e., the maximum central deflection of the nanoplate.

Nanoplates having different shapes (e.g., rectangular) and boundary conditions (e.g., fixed) can be treated in the same manner (see next section). For a nanoplate equation (5) becomes (see, for example, [**12**])

$$E_{\text{elast-b}} = \frac{D}{2}\int_S \{k_{xx}^2 + k_{yy}^2 + 2\nu k_{xx}k_{yy} + 2(1-\nu)k_{xy}^2\}\,\mathrm{d}x\,\mathrm{d}y \tag{26a}$$

$$E_{\text{elast-m}} = \frac{Et}{2(1-\nu^2)}\int_S \{\varepsilon_{xx}^2 + \varepsilon_{yy}^2 + 2\nu\varepsilon_{xx}\varepsilon_{yy} + 2(1-\nu)\varepsilon_{xy}^2\}\,\mathrm{d}x\,\mathrm{d}y \tag{26b}$$

$$k_{xx} = w_{,xx}, \quad k_{yy} = w_{,yy}, \quad k_{xy} = w_{,xy},$$
$$\varepsilon_{xx} = u_{,x} + \tfrac{1}{2}w_{,x}^2, \varepsilon_{yy} = v_{,y} + \tfrac{1}{2}w_{,y}^2,$$
$$\varepsilon_{xy} = \frac{u_{,y} + v_{,x} + w_{,x}w_{,y}}{2} \tag{26c}$$

Equation (26a) corresponds to the bending regime and equation (26b) to the membrane regime of the nanoplate and $E_{\mathrm{elast}} = E_{\text{elast-b}} + E_{\text{elast-m}}$. These expressions are only functions of the displacements as reported in equation (26c). The term of equation (26b) describing the finite kinematics of the

nanoplate is significant only in the description of large displacements and when the boundary conditions impose the stretching of the nanoplate. It is expected that $E_{\text{elast-m}} \propto E_{\text{elast-b}} c^2/t^2$ [**4**]; thus, focusing the attention to moderate displacements the energy related to the membrane regime can be neglected.

Owing to the structure and load axial symmetry, and neglecting the role of the membrane regime, in polar coordinates equation (26a) is rewritten as

$$E_{\text{elast}} = \frac{D}{2}\int_0^R \left\{ \left(w_{,\rho\rho} + \frac{w_{,\rho}}{\rho} \right)^2 - 2(1-\nu)\frac{w_{,\rho\rho} w_{,\rho}}{\rho} \right\} \times 2\pi\rho \, \mathrm{d}\rho \tag{27}$$

from which, introducing equation (25)

$$E_{\text{elast}} = \frac{4\pi D(1+\nu)}{R^2} c^2 \tag{28}$$

On the other hand, the electrostatic and van der Waals energies can be computed as

$$E_{\text{elec,vdW}} = \int_S \frac{\mathrm{d}E_{\text{elec,vdW}}}{\mathrm{d}S} \, \mathrm{d}S \tag{29}$$

The integrations of equations (27) and (29) can be done directly in w noting that equation (25) implies $\mathrm{d}S = 2\pi\rho \, \mathrm{d}\rho = -\pi R^2/c \, \mathrm{d}w$; the results are

$$E_{\text{elec}} = \frac{\varepsilon_0 \pi R^2 V^2}{H} \left\{ \frac{1}{2} + \frac{1}{4}\frac{c}{H} + \frac{1}{6}\left(\frac{c}{H}\right)^2 \right\} \tag{30}$$

$$E_{\text{vdW}} = \frac{\pi^2 C_6 n^2 R^2 t}{H^3} \left\{ \frac{1}{6} + \frac{1}{4}\frac{c}{H} + \frac{1}{3}\left(\frac{c}{H}\right)^2 \right\} \tag{31}$$

Applying equation (7) we find

$$c = \frac{3\varepsilon_0 R^4 H^3 V^2 + 3\pi R^4 C_6 n^2 t H}{8Et^3 H^5/(1-\nu) - 4\varepsilon_0 R^4 H^2 V^2 - 8\pi R^4 C_6 n^2 t} \tag{32}$$

whereas equation (8) gives the pull-in voltage (i.e. the switch) of the device

$$V_{\text{PI}} = \sqrt{\frac{2Et^3 H^5/(1-\nu) - 2\pi C_6 R^4 n^2 t}{\varepsilon_0 R^4 H^2}} \tag{33}$$

The condition for which the numerator of equation (33) becomes zero corresponds to the structural instability simply owing to the van der Waals forces and it will be reached when the following dimensionless number α reaches the unity

$$\alpha = \frac{\pi(1-\nu) C_6 n^2 R^4}{Et^2 H^5} \tag{34}$$

For large gaps H (e.g., larger than $\sim$10 nm) the van der Waals forces can be neglected and equations (32) and (33) become respectively

$$c = \frac{3\varepsilon_0 R^4 H V^2}{8E/(1-\nu) t^3 H^3 - 4\varepsilon_0 R^4 V^2}$$

and

$$V_{\text{PI}} = \sqrt{\frac{2Et^3 H^3}{(1-\nu)\varepsilon_0 R^4}}$$

Scaling each characteristic length of the system by a factor of l, the pull-in voltage of the nanoplate scales as $V_{\text{PI}} \propto l$, as for nanotubes [**10**]. Including also the membrane regime would correspond to $V_{\text{PI-m}} \approx \sqrt{1+k_{\text{m}}} V_{\text{PI}}$, with $k_{\text{m}} \propto H^2/t^2$ that can be derived from equation (26) assuming a given mode-shape for the deflection w, as in equation (25).

6.2 Rectangular nanoplates or nanowires

Rectangular nanoplates can be treated at the same manner, and the corresponding equations hold also for nanowires with rectangular cross-section $B \times t$. For cantilever nanoplate/nanowire of length L (clamped at $x = 0$), we can assume an elastic line of the form

$$w(x,y) = w(x) \approx c \, \frac{x^2}{L^2} \tag{35}$$

By applying equations (26a) and (29) we obtain [from equation (35), $\mathrm{d}S = (BL/2)\,(\mathrm{d}w/\sqrt{wc})$]

$$E_{\text{elast}} = \frac{2DB}{L^3} c^2 \tag{36a}$$

$$E_{\text{elec}} = \frac{\varepsilon_0 BL V^2}{H} \left\{ \frac{1}{2} + \frac{1}{6}\frac{c}{H} + \frac{1}{10}\left(\frac{c}{H}\right)^2 \right\} \tag{36b}$$

$$E_{\text{vdW}} = \frac{\pi C_6 n^2 BLt}{H^3} \left\{ \frac{1}{6} + \frac{1}{6}\frac{c}{H} + \frac{1}{5}\left(\frac{c}{H}\right)^2 \right\} \tag{36c}$$

Applying equation (7) we find

$$c = \frac{5\varepsilon_0 L^4 H^3 V^2 + 5\pi L^4 C_6 n^2 t H}{10Et^3 H^5/(1-\nu) - 6\varepsilon_0 L^4 H^2 V^2 - 12\pi L^4 C_6 n^2 t} \tag{37}$$

whereas equation (8) gives

$$V_{\text{PI}} = \sqrt{\frac{5Et^3 H^5/(1-\nu) - 6\pi C_6 L^4 n^2 t}{3\varepsilon_0 L^4 H^2}} \tag{38}$$

and for vanishing van der Waals forces

$$V_{\text{PI}} \approx \zeta \sqrt{\frac{Et^3 H^3}{(1-\nu)\varepsilon_0 L^4}}$$

with ζ close to unity (considering only the first two significant terms in the energy expansions $\zeta \approx 1.3$). Assuming a rigid plate connected to the substrate by a concentrated stiffness, as is usually done to model MEMS, since for the cantilever the stiffness is expected to be $8EI/L^3$ (here a constant force per unit length is assumed), with I inertia moment, this simple model would correspond to the same formula of equation (38) with $\zeta \approx 0.45$ (and $\nu \approx 0$) [**10**]. This comparison shows that the approach is consistent. Considering additional terms in the energy expansion as well as more appropriate forms for the deflection w would correspond to a better estimation for ζ. Rigorously, the coefficient ζ could be considered a numerical (derived from just one simulation; or experimental) parameter as a correction to the simplified hypotheses. However, ζ is expected to be of the order of the unity as suggested by the analysis. This comparison in addition shows that the analysis can be applied also for MEMS based on micro-plates and beams; because $F_{\text{vdW}} \propto q_{\text{vdW}} l^2 \propto l^{-1}$, increasing the size l of the NEMS device by three orders of magnitude as for MEMS, the van der Waals forces become negligible.

Including also the membrane regime would correspond to $V_{\text{PI-m}} \approx \sqrt{1 + k_{\text{m}}} V_{\text{PI}}$, with $k_{\text{m}} \propto H^2/t^2$; the coefficient of proportionality can be derived from equations (26) assuming a given modeshape for the deflection w, as in equation (35), or more precisely from one numerical simulation.

7 DYNAMICS OF THE NANOPLATE-BASED NEMS

The static configuration w_{S} (the subscript S emphasises that it is related to statics) is assumed to be given by equation (25) (or by an equivalent form for different shapes and/or boundary conditions, e.g., equation (35)). The vibrations around the deformed configuration w_{S} (the solution obtained by minimizing the free energy in section 6) are

$$w_{\text{D}}(x, y, t) \approx w_{\text{S}}(x, y) + \Delta w_{\text{D}}(x, y, t) \tag{39}$$

where w_{D} is the dynamic deflection of the nanoplate and Δw_{D} is the time-dependent component of w_{D}. For the fundamental frequency

$$\Delta w_{\text{D}}(x, y, t) \approx \frac{w_{\text{S}}(x, y)}{c_{\text{S}}} c_{\text{D}}(t) = \frac{w_{\text{S}}(x, y)}{c_{\text{S}}} c_{\text{D}}^* \sin(\omega t) \tag{40}$$

where c_{S} is the static displacement at the equilibrium and c_{D}^* represents the maximum amplitude of the harmonic oscillations around the equilibrium position c_{S}. The kinetic energy of the system will thus be

$$\begin{aligned} K(t) &= \frac{1}{2} \int_M \left(\frac{\mathrm{d}w_{\text{D}}(x, y, t)}{\mathrm{d}t} \right)^2 \mathrm{d}M \\ &= \frac{\mu}{2} \int_S \left(\frac{\mathrm{d}\Delta w_{\text{D}}(x, y, t)}{\mathrm{d}t} \right)^2 \mathrm{d}S \end{aligned} \tag{41}$$

where M is the mass of the nanoplate (μ is the mass per unit area).

Putting equation (40) into equation (41) and considering a circular (equation (25)) or rectangular nanoplate (equation (35)), gives

$$K(t) = \tfrac{1}{2} m_{\text{eq}} c_{\text{D}}^{*2} \omega^2 \cos^2(\omega t) \tag{42}$$

where for a circular nanoplate $m_{\text{eq}}^{(\text{C})} = 1/3M$ and for a rectangular nanoplate $m_{\text{eq}}^{(\text{R})} = 1/5M$ (everywhere the superscript (C) will refer to circular and (R) to rectangular nanoplates).

From the previous considerations for the quasi-static regime, the free energy is

$$W(c) = E_{\text{elast}}(c) - E_{\text{elec}}(c) - E_{\text{vdW}}(c) \tag{43}$$

where according to equations (39) and (40)

$$c = c_{\text{S}} + c_{\text{D}}^* \sin(\omega t) \tag{44}$$

Let the reference system of the energy be fixed as $W(c_{\text{S}}) = 0$. In this hypothesis the maximum free energy and the maximum kinetic energy of the NEMS must be the same. The fundamental frequency ω is thus estimated as

$$\omega = \sqrt{\frac{2W(c)|_{\max}}{m_{\text{eq}} c_{\text{D}}^{*2}}} \tag{45}$$

From the quasi-static analysis, the form of $W(c)$ is known. If the kinetic energy of the system is known, from equations (45) and (42) the dynamic displacement c_{D}^* can be estimated.

If the oscillations are small, according to equation (9), the free energy is estimated as

$$\begin{aligned} W(c) &\cong \frac{1}{2} \frac{\mathrm{d}^2 W(c)}{\mathrm{d}c^2}\bigg|_{c=c_{\text{S}}} (c - c_{\text{S}})^2 \\ &= \frac{1}{2} \frac{\mathrm{d}^2 W(c)}{\mathrm{d}c^2}\bigg|_{c=c_{\text{S}}} (c_{\text{D}}^* \sin(\omega t))^2 \end{aligned} \tag{46}$$

Introducing the maximum value of equation (46) into equation (45), the rotating frequency is predicted to be

$$\omega = \sqrt{\frac{1}{m_{\text{eq}}} \frac{\mathrm{d}^2 W(c)}{\mathrm{d}c^2}\bigg|_{c=c_{\text{S}}}} \tag{47}$$

not dependent on the amplitude c_{D}^* but on the

external fields (e.g., the electrical field and the van der Waals forces) as the second derivative of the free energy. If the oscillations are not small the frequency will be a function also of their amplitude (equation (45)).

7.1 Free oscillations

For free vibrations

$$W = E_{\text{elast}} \tag{48}$$

as given by equations (28) and (36a). From equation (47), for circular and rectangular nanoplates the fundamental (free) frequencies are

$$\omega^{(\text{C})} = \sqrt{\frac{8\pi(1+\nu)D}{R^2 m_{\text{eq}}}} \tag{49a}$$

$$\omega^{(\text{R})} = \sqrt{\frac{4DB}{L^3 m_{\text{eq}}}} \tag{49b}$$

The ratio between the exact solution of the fundamental frequency for a cantilever beam and that predicted by equation (49b) is 0.8 (assuming the beam as a cantilever nanoplate with negligible Poisson's ratio), a coefficient close to unity. Thus, the theory is consistent.

7.2 Thermal vibrations

For thermal vibrations, the equipartition theorem implies a mean value of the kinetic energy

$$\langle K(\tau)\rangle = \frac{1}{P}\int_P K(\tau)\,\mathrm{d}\tau = \frac{k_{\text{B}}T}{2} \tag{50}$$

where $P = 2\pi/\omega$ is the period of the oscillation and k_{B} is Boltzmann's constant. Putting equations (50) and (48) into the mean value of equation (42) gives the amplitude c_{D}^* of the thermal vibration around the position described by c_{S}

$$c_{\text{D}}^* = \sqrt{\frac{2k_{\text{B}}T}{\left.\dfrac{\mathrm{d}^2 W(c)}{\mathrm{d}c^2}\right|_{c=c_{\text{S}}}}} \tag{51}$$

The frequency is given by equation (47).

For free oscillations, the equipartition theorem applied to the higher modes m fixes their relative amplitudes, that fall off as $\sim 1/m^2$. Hence, the vibration amplitude profile is dominated by the first mode.

7.2.1 Relaxed configuration

Considering the thermal vibrations around a relaxed configuration, introducing equations (28) and (36a) into equation (51) yields

$$c_{\text{D}}^{*(\text{C})} = \sqrt{\frac{R^2 k_{\text{B}}T}{4\pi D(1+\nu)}} \tag{52a}$$

$$c_{\text{D}}^{*(\text{R})} = \sqrt{\frac{L^3 k_{\text{B}}T}{2DB}} \tag{52b}$$

and ω is given by equations (49).

7.2.2 Deformed configuration

From equations (30), (31), (36b), and (36c) we obtain

$$\frac{\mathrm{d}^2 E_{\text{elec}}}{\mathrm{d}c^2} = \frac{m_{\text{eq}}}{\mu}\frac{\varepsilon_0 V^2}{H^3} \tag{53}$$

$$\frac{\mathrm{d}^2 E_{\text{vdW}}}{\mathrm{d}c^2} = \frac{2\pi C_6 n^2 t m_{\text{eq}}}{\mu H^5} \tag{54}$$

so that from equations (47) and (51) the frequency and amplitude satisfy

$$\omega_{\text{V}}^{(\text{C,R})} = \left(\omega^{(\text{C,R})2} - \frac{\varepsilon_0 V^2}{\mu H^3} - \frac{2\pi C_6 n^2 t}{\mu H^5}\right)^{1/2} \tag{55}$$

$$c_{\text{DV}}^{*(\text{C,R})} = \left(\frac{1}{c_{\text{D}}^{*(\text{C,R})2}} - \frac{\varepsilon_0 V^2 m_{\text{eq}}}{2\mu H^3 k_{\text{B}}T} - \frac{\pi C_6 n^2 t m_{\text{eq}}}{\mu H^5 k_{\text{B}}T}\right)^{-1/2} \tag{56}$$

where the subscript V emphasizes the influence of the electrical field. According to equation (55) the pull-in instability (displacement tending to infinity) can be obtained also by setting $\omega_{\text{V}}^{(\text{C,R})} = 0$, thus $\mathrm{d}^2 W(c)/\mathrm{d}c^2|_{\text{PI}} = 0$. Approaching the pull-in, the amplitude of the thermal vibrations will increase, and their frequencies will decrease. Practically, when they become large enough, the approximation of small vibrations is no longer valid and the amplitude will be limited. The kinetic energy released after the pull-in can be evaluated as the difference between the free energy (exact form) at the pull-in and at the contact, i.e. $K_{\text{PI}} = W_{\text{PI}} - W_{\text{cont}}$.

7.3 Schrödinger's equation: the oscillations imposed by Heisenberg's principle

The Hamiltonian of the NEMS can be written as ($W(c_{\text{S}}) = 0$)

$$H(c,t) = K(c,t) + W(c) \tag{57}$$

Schrödinger's equation takes a simple form as a consequence of the reduction to one degree of freedom of the system as

$$\left(-\frac{\hbar^2}{2m_{\text{eq}}}\frac{\partial^2}{\partial c^2} + W(c)\right)\psi_n(c) = E_n\psi_n(c) \tag{58}$$

where E_n are the energy eigenvalues and ψ_n are the eingenfunctions describing the fundamental vibrational states. Equation (58) can be solved numerically. For small dynamic displacements around a deflected configuration and substituting the conditions of equations (46) and (47) yields the (well-known) discrete quantized levels of energy

$$E_n \approx (\tfrac{1}{2} + n)\hbar\omega \tag{59}$$

Note that here ω is not the fundamental frequency of the free NEMS but, according to equation (47), takes into account the electrical field and van der Waals forces. Obviously, the lowest energy level is predicted to be different from zero also at zero temperature

$$E_0 \approx \frac{\hbar\omega}{2} \tag{60}$$

as imposed by Heisenberg's uncertainty principle.

The condition for which equation (50) equals equation (60) corresponds to the temperature for which the vibration of the zero point becomes equal to the thermal vibrations

$$k_B T \approx \hbar\omega \tag{61}$$

According to equation (60), the corresponding amplitude of the zero point can be obtained as

$$c^*_{D0} = \sqrt{\frac{2\hbar}{\sqrt{m_{eq}\left.\dfrac{d^2 W(c)}{dc^2}\right|_{c=c_S}}}} \tag{62}$$

The corresponding frequency is given by equation (49) and consequently

$$c^{*(C)}_{D0} = \sqrt{\frac{R\hbar}{\sqrt{2\pi D(1+\nu)m_{eq}}}} \tag{63a}$$

$$c^{*(R)}_{D0} = \sqrt{\frac{L^{3/2}\hbar}{\sqrt{DBm_{eq}}}} \tag{63b}$$

8 AN EXAMPLE OF APPLICATION

As an example of application of the developed approach, some results for a circular carbon graphene sheet ($t = 0.335$ nm) assuming $R = 10$ nm, $H = 3$ nm, $E = 1$ TPa, $\nu = 0$, $V = 1$ V, and $T = 300$ K (if not differently specified), over a semi-infinite bulk-graphite substrate are reported in Figs 2 to 4 for the statics, and in Figs 5 to 7 for the dynamics of the NEMS. The structural behaviours described by the grey lines take into account the van der Waals forces. On the other hand, the black lines describe structural behaviours without considering van der Waals forces.

The pull-in voltages as a function of the horizontal R and vertical H sizes of the NEMS are depicted in Figs 2 and 3. When H reaches a lower bound, which for the considered geometry is ~1.5 nm, the nanoplate collapses owing to the van der Waals forces and the pull-in voltage vanishes. Increasing the initial gap H, the van der Waals corrections tend to become negligible and the two different lines in Fig. 2 tend to coincide. For $R = 10$ nm and $H = 3$ nm, the pull-in voltage is ~4.7 V.

In Fig. 4, the central deflection c of the carbon nanoplate versus the applied voltage V is reported. For the grey line the deflection corresponding to a vanishing applied voltage represents the central displacement of the nanoplate owing to the van der Waals attraction. In general, van der Waals forces increase the nanoplate deflections.

In Fig. 5 the frequency of the oscillations around the equilibrium static position (described in Fig. 3) is reported as a function of the applied voltage. The frequency becomes negligible at the pull-in. Van der Waals forces and the applied voltage reduce the fundamental frequency. Thus, by controlling the voltage, the operating frequency of the NEMS could be controlled (e.g., perhaps useful for 'smart' mass sensors and accelerometers, etc.).

In Figs 6 and 7 the amplitude of the oscillations is shown as a function of the applied voltage (at 300 K)

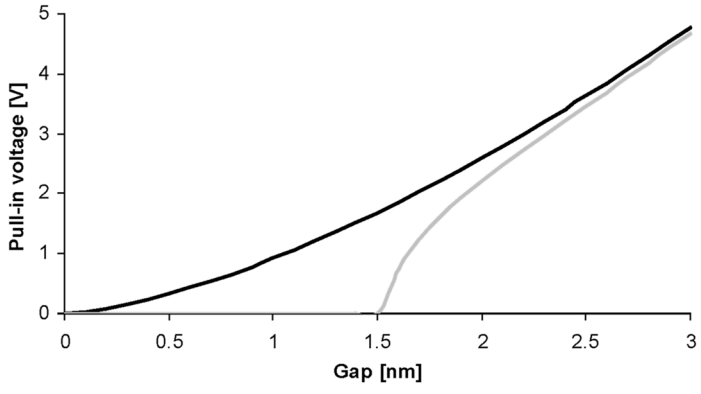

Fig. 2 Pull-in voltage versus vertical size (nominal gap) between nanoplate and plane. Grey line: with van der Waals forces; black line: without

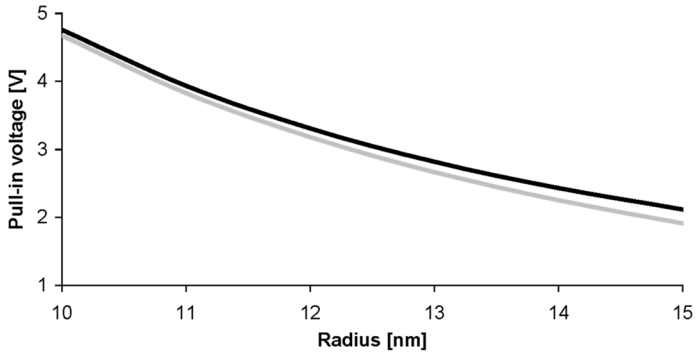

Fig. 3 Pull-in voltage versus horizontal gap (nanoplate radius). Grey line: with van der Waals forces; black line: without

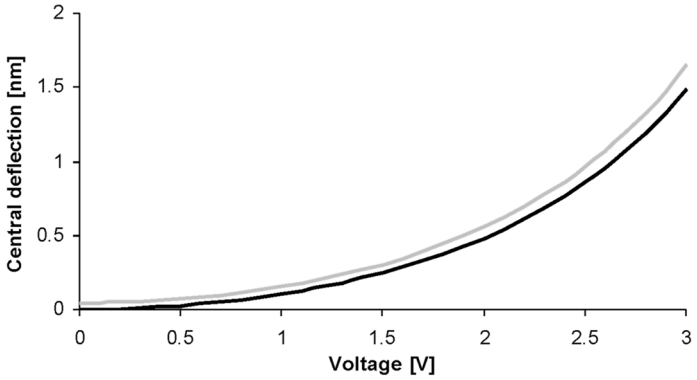

Fig. 4 Central deflection of the nanoplate versus applied voltage. Grey line: with van der Waals forces; black line: without

and temperature (under 1 V). In Fig. 7, the horizontal lower line represents the amplitude of the oscillations imposed by the Heisenberg's principle.

The van der Waals forces and applied voltage increase the amplitude of the oscillations. By controlling the voltage, NEMS with variable 'global' stiffness, also tending to zero could be designed (e.g., perhaps useful for highly sensitive temperature sensors, capable to 'observe' the energy of the zero point).

At zero voltage, the frequency $P^{-1} = \omega/(2\pi)$ of the dominant mode of the thermal oscillations is $\sim$16 GHz. The amplitude of the thermal oscillations at 300 K is $\sim$1 Å, whereas the zero-point oscillation is $\sim$0.05 Å.

Here a *voltage control* has been assumed resulting, as shown, in a *digital* NEMS. Digital NEMS, owing to their high integration level and operating frequency, could revolutionize the electronic components of the future, e.g., nanoswitches for computer memory applications. On the other hand, a complementary *current control* could be also proposed, as a consequence of the quantum tunnelling effect. This

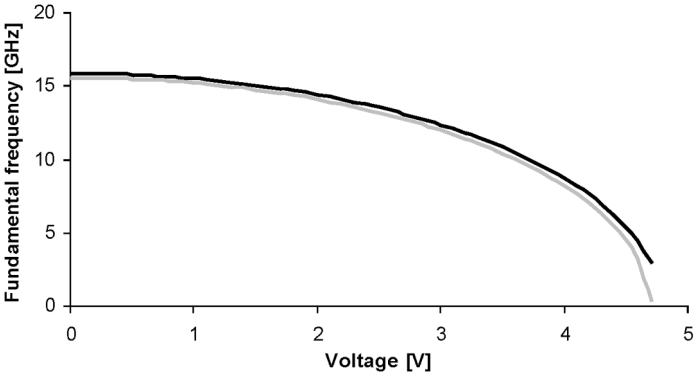

Fig. 5 Fundamental frequency of the nanoplate versus applied voltage. Grey line: with van der Waals forces; black line: without

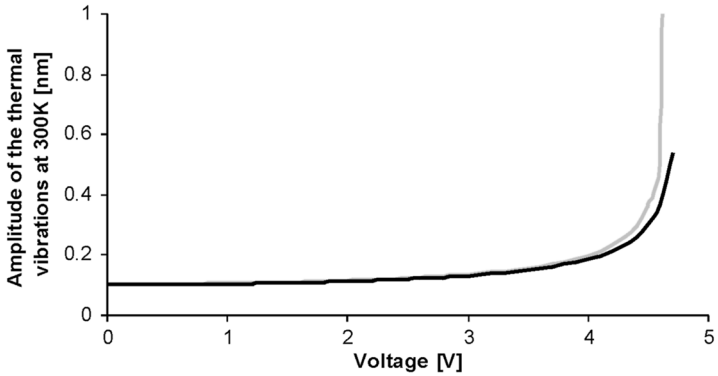

Fig. 6 Amplitude of the thermal vibrations (300 K) versus applied voltage. Grey line: with van der Waals forces; black line: without

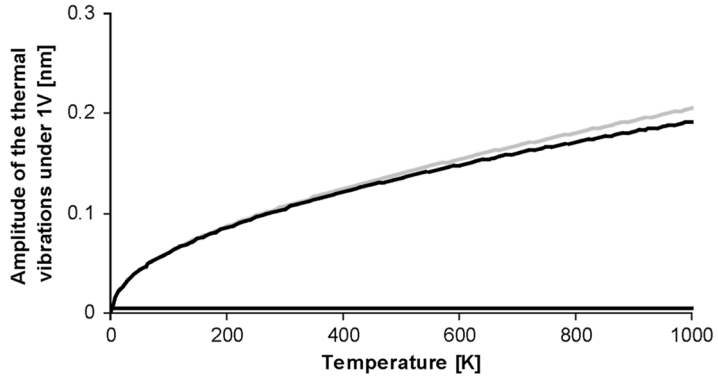

Fig. 7 Amplitude of the thermal vibrations versus temperature. Grey line: with van der Waals forces; black line: without; under an applied voltage of 1 V. The horizontal lower line represents the amplitude of the oscillations imposed by the Heisenberg's principle

would result, at least for small gaps, in a current between the NEMS (especially for cantilever nanowires (or nanotubes, see [**14**, **15**]), possessing a sharp tip) and electrode with intensity related to the smaller gap between the NEMS and electrode. Thus, imposing a current would correspond to an *analogical* NEMS (perhaps useful for innovative microscope tips, electron counters, etc.).

9 CONCLUSION

The statics and dynamics of three-dimensional NEMS have been analysed. The elastic equilibrium of a nanoplate (or nanowire) under electrostatic and van der Waals forces and suspended over a grounded semi-infinite plane has been analysed for the static and dynamic regimes (for a similar analysis of nanotubes see [**4**]). The equilibrium position was obtained by minimizing the total free energy of the nanoplate- (or nanowire-) based NEMS. In addition, the structural instability owing to the pull-in voltage has been theoretically predicted. In contrast to other analytical analyses the presented approach considers the flexibility of the system in evaluating the elastic and van der Waals energies. A simple approach to estimate the amplitude and the frequency of the thermal vibrations by applying the equipartition theorem, has been also proposed. In contrast to other analytical analyses the presented approach considers vibrations around a generic deformed configuration, i.e. the influence of the applied voltage and van der Waals forces in the dynamics of the NEMS. The zero-point oscillations, as imposed by the Heisenberg's principle, have also been evaluated. This work is meant as a step towards an optimal dynamical design paradigm for three-dimensional NEMS(/MEMS).

ACKNOWLEDGEMENTS

The author would like to thank Professors A. Carpinteri and R. S. Ruoff, H. D. Espinosa, and N. Moldovan for many insightful discussions.

REFERENCES

1 **Kim, P.** and **Lieber, C. M.** Nanotube nanotweezers. *Science*, 1999, **286**, 2148–2150.

2 **Baughman, R. H., Changxing Cui, Zakhidov, A. A., Iqbal, Z., Barisci, J. N., Spinks, G. M., Wallace, G. G., Mazzoldi, A., De Rossi, D., Rinzler, A. G., Janchinski, O., Roth, S.,** and **Kertesz, M.** Carbon nanotube actuators. *Science*, 1999, **284**, 1340–1344.

3 **Rueckes, T., Kim, K., Joselevich, E., Tseng, G. Y., Cheung, C.-L.,** and **Lieber, C. M.** Carbon nanotube-based nonvolatile random access memory for molecular computing. *Science*, 2000, **289**, 94–97.

4 **Pugno, N.** Non-linear dynamics of nanotube based NEMS. *Rec. Res. Dev. Sound Vibr.*, 2004, **2**, 197–211.

5 **Qian, D., Wagner, G. J., Liu, W. K., Yu, M.-F.,** and **Ruoff, R. S.** Mechanics of carbon nanotubes. *Appl. Mech. Rev.*, 2002, **55**, 495–532.

6 **Iijima, S.** Helical microtubules of graphitic carbon. *Nature*, 1991, **354**, 56–58.

7 **Pugno, N.** and **Ruoff, R.** Quantized fracture mechanics. *Phil. Mag.*, 2004, **84**, 2829–2845.

8 **Yakobson, B. I.** and **Smalley, R. E.** Fullerene nanotubes: C-1000000 and beyond. *Am. Scient.*, 1997, **85**, 324–337.

9 **Girifalco, L. A.** Molecular properties of C60 in the gas and solid phases. *J. Phys. Chem.*, 1992, **96**, 858–861.

10 **Dequesnes, M., Rotkin, S. V.,** and **Alaru, N. R.** Calculation of pull-in voltages for carbon-nanotube-based nanoelectromechanical switches. *Nanotechnology*, 2002, **13**, 120–131.

11 **Chopra, N. G.** and **Zettl, A.** Measurement of the elasticity of a multi-wall boron nitride nanotube. *Solid State. Comm.*, 1998, **105**, 297–300.

12 **Carpinteri, A.** *Structural mechanics – a unified approach*, 1997 (E & FN Spon, New York).

13 **Bazant, Z. P.** and **Cedolin, L.** *Stability of structure: elastic, inelastic, fracture and damage theories*, 1991 (Oxford University Press, Oxford).

14 **Pugno, N.** Tunneling current/voltage control, oscillations and instability of nanotube and nanowire based NEMS. *Glass Phys. Chem.*, Special Issue: Nanoparticles, Nanostructures and Nanocomposites, 2004, **31**, 535–544.

15 **Ke, C. H., Espinosa, H. D.,** and **Pugno, N.** A feedback controlled carbon nanotube based NEMS device, International Conference on *Experimental Mechanics-12*, CD-ROM (No. 81), 29 August–2 September, 2004, Bari, Italy.

APPENDIX

Notation

B	width of the nanowire
$c_{\mathrm{D}i}$	unknowns dynamic displacements
c_i	unknowns static displacements
C	electrical capacitance
D	nanoplate rigidity
E, ν	Young's modulus and the Poisson's ratio
$E_{\mathrm{elast,elec,vdW,P}}$	elastic, electrostatic, van der Waals and Pauli's energies
E_{in}	energy eigenvalues
$F_{\mathrm{elec,vdW,P}}$, $q_{\mathrm{elec,vdW,P}}$	electrostatic, van der Waals and Pauli's forces F, and q if per unit area S
$[\mathrm{H_W}]$	Hessian matrix of the free-energy
K	kinetic energy
L	length of the nanowire
m_{eq}	equivalent mass of the nanoplate/nanowire
m_i	modal mass
$[\mathrm{M}]$	mass matrix
M	mass of the nanoplate/nanowire
$n_{1,2}$	atom densities
r, H	gaps in the deformed and undeformed configurations
R	radius of the nanoplate
t	nanoplate thickness; $D = Et^3/12(1-\nu^2)$
T	temperature
u_i, v_i, w_i	displacements
V	difference in voltage
$W(c_i)$	free energy
ψ_{in}	Eigenfunctions
ω	fundamental frequency